

10,11

Effect of the size of nanocrystalline zinc oxide particles on the conductance of aminated graphene

© P.V. Barkov¹, O.E. Glukhova^{1,2,¶}

¹ Department of Physics, Saratov State University, Saratov, Russia

² Institute of Bionic Technologies and Engineering, Sechenov First Moscow State Medical University of Ministry of Health of Russia, Moscow, Russia

¶ E-mail: glukhovaoe@info.sgu.ru

Received June 19, 2024

Revised July 4, 2024

Accepted July 4, 2024

By method of density functional we determined nature and degree of effect of size of ZnO-nanocrystals on the fermi energy, profile of density function of electron states and conductance of aminated graphene (AmGr). It was determined that localization of ZnO-nanocrystals near NH₂-groups with formation of covalent bonds of nanocrystals with AmGr by formation of Zn–N-bonds is energy favorable. increase in size of ZnO-nanocrystals from sub- to nanometer size results in resistance increasing by three times, this makes such films promising for the sensing of water and gas molecules.

Keywords: ZnO-nanocrystals, conductance, Fermi level, transmittance function of electrons, density of electron states, functionalized graphene.

DOI: 10.61011/PSS.2024.08.59063.159

1. Introduction

The graphene modification allows control of its physical properties, including electronic properties and electrical conductivity. One of the effective ways of graphene modification is amination (process of graphene functionalization by aminogroups NH₂) and decoration by nanocrystals of zinc oxide. For practical tasks the functionalization of the basal plane of the graphene with formation of sp³-bonds in carbon atoms is important. The graphene decoration by aminogroups changes its electronic structure, in particular, ensures control of electrons work function [1], at that on band structure there is energy slot band gap ~ 0.1 eV. Currently the aminated graphene (AmGr) is assumed as promising material for different applications in photovoltaics, gas and biosensors, drug delivery and new composites [2–5]. Different strategies of amine functionalization of the graphene are used. For example, aminogroups are „stitched on“ using electron beam [6]. It was determined by experiments that the functional groups sit on both edge atoms of the graphene, and on its basal plane. The sitting process and its patterns are studied also using computer modeling [7–10]. For example, paper [7] relates to detail analysis of different approaches to modeling of the graphene functionalization. This paper is a kind of road map for all who are engaged in such issues. Note that in paper [7] the functionalization modeling is performed by different quantum-mechanical methods: empiric, semi-empiric and method of density functional. Papers [8–10] demonstrate models of functionalized graphene obtained by method of density functional, although along with this

method the empiric approaches are used to simulate the process of surface functionalization of graphene-polymer nanocomposites [11], and finite element methods to study new properties of functionalized graphene nanoplates [12].

Some patterns of graphene functionalization by various groups are identified. For example, it is identified that basic oxygen-containing functional groups, most frequently decorating the graphene, are epoxides (C–O–C), phenolic hydroxyls (–OH), carboxyl (–COOH) and other carbonyl groups (C=O). At that carboxyl (–COOH) groups are mainly located at edges, and phenolic hydroxyl (–OH) and epoxide (C–O–C) groups — on basal surface of the graphene [13–15].

Other widely used functionalizing groups are groups comprising nitrogen, sulfur, fluorine and other nonmetal elements [16–18]. This paper authors determine in advance the patterns of aminogroups adhering to basal surface of graphene [19]: 1) for groups it is energy favorable to adhere along trajectory „zigzag“ to the basal surface of the graphene; 2) successively in direction „zigzag“ sitting of only eleven NH₂-groups is possible. As result of optimization it was identified, that adherence of 12-th aminogroup results in break of the atomic grid of the graphene with nanohole formation. Due to this exactly AmGr is discussed in this paper. Already aminated graphene can be also modified, for example, decorated by nanocrystals of zinc oxide. Nanoparticles/nanocrystals of zinc oxide (ZnO) during last years become very promising due to their use in optics, optoelectronics, sensorics, energetics and biomedicine due to the wide availability of these nanoparticles, their low

production cost and environmental friendliness [20–22]. Currently ZnO-nanocrystals of different dimensions are synthesized, including nanometer and even subnanometer. Most frequently crystals of zinc oxide are synthesized with hexagonal crystal lattice (symmetry group P63mc). At that four crystallographic phases of surfaces are identified: non-polar ZnO (10 $\bar{1}0$) and ZnO (11 $\bar{2}0$), and polar with plane „zinc“ ZnO (0001) and plane „oxygen“ Zn (000 $\bar{1}$). The non-polar surfaces of greatest interest [23–26].

This paper task is to determine patterns of size effect of nanocrystals ZnO on electronic properties and conductivity of AmGr.

2. Method of study

Atomistic modeling of zinc oxide nanoparticles and AmGr supercells was performed using the density functional method in the tight-binding approximation. Exactly this method implemented in software package DFTB+ [27] was previously used to obtain the equilibrium super-cells AmGr [19].

Interaction of C, N, O, H-atoms is described by the basis set of parameters pbc-0-3 [27] for solid-state structure, and interaction of Zn-atoms with C, N, O, H-atoms — using basis set of znorg-0-1 [27]. The dispersive interaction of nanoparticles with AmGr was also considered. To obtain energy favorable atomic configuration of super-cells AmGr and zinc oxide particles the full energy minimization was performed by all coordinates of all atoms, and by all lengths of translation vector of super-cell at electron temperature 300 K. Like in all similar calculations, 3D-periodic box with size at axis Z (perpendicular to surface AmGr) 500 Å was used. To study the atomic structure of zinc oxide particles 3D-periodic box with size 500 × 500 × 500 Å was used. When modeling complex „nanoparticle ZnO+AmGr“ Monkhorst–Pack approach was used to divide the first Brillouin zone, at that grid 4 × 4 × 1 was used. To minimize full energy the conjugate gradients method was used. Condition for full energy minimum achievement was force acting on atom, its value shall not exceed 10⁻⁴ eV/atom.

Conductivity was calculated Using the following formula

$$G = \frac{2e^2}{h} \int_{-\infty}^{\infty} T(E, k) F_T(E - E_F) dE, \quad (1)$$

where $T(E, k)$ — electron transmittance function, E — energy, k — wavenumber, F_T — function determining temperature broadening of energy levels, E_F — Fermi energy of contacts, e — electron charge, h — Planck's constant, $2e^2/h$ — value of conductance quantum for doubled to consider spin. The electron transmittance function is determined by expression

$$T(E) = \text{Tr}(\Gamma_S(E) G_C^A(E) \Gamma_D(E) G_C^R(E)), \quad (2)$$

where $G_C^A(E)$, $G_C^R(E)$ — advanced and retarded Green's matrices describing the contact with electrodes, $\Gamma_S(E)$,

$\Gamma_D(E)$ — energy level broadening matrices for the source and drain. Function determining the temperature broadening of energy levels is written as follows:

$$F_T(E) = \frac{1}{4k_B T} \text{sech}^2\left(\frac{E}{2k_B T}\right), \quad (3)$$

where k_B — Boltzmann constant, T — temperature.

Function $T(E, k)$ determines number of conductivity channels or, more accurately, the degree of transparency for electrons passing through the structure under study. As a rule, for each value of energy averaging is performed along all wavenumbers from first Brillouin zone. The transparency function was calculated using instrument of Green–Keldysh nonequilibrium function, as well as Landauer–Buttiker formalism, which ensures study of the electron transport considering elastic scattering of electrons by defects [28,29].

3. Results

3.1. Atomistic models of ZnO nanoparticles of subnanometer size

Studies of energy characteristics of ZnO nanoparticles of different topology showed that most energy favorable nanoparticles are those in which maximum surface is presented by Miller indices (001). The nanoparticle with minimum stability is structure of 6 atoms, see Figure 1, *a*. It comprises three zinc atoms and three oxygen atoms; other particles comprise 12 (double minimum particle, Figure 1, *b*), 48 and 96 atoms (Figure 1, *c* and *d*). All particles have symmetric configuration, this is confirmed by density distribution of electron charge by atoms (Figure 2). Excessive negative charge is observed on oxygen atom — $\sim -0.6|e|$ (designated by blue color), same positive charge (lack of charge) — on zinc atoms (designated by red color). As number of atoms increases in nanoparticle the full energy decreases from value -104.8837 to -105.8179 eV/atom, Fermi energy at that changes insignificantly, from -4.12 to -3.99 eV respectively. Density distribution of electron charge also slightly changes: upon increase in number of

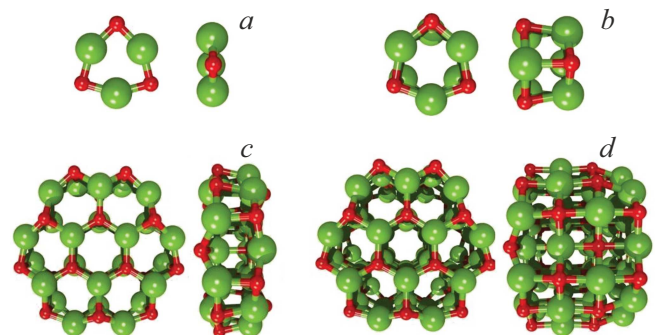


Figure 1. Atomistic models of zinc oxide nanoparticles: *a*) 6 atoms, *b*) 12 atoms, *c*) 48 atoms, *d*) 96 atoms (large green balls designate zinc atoms, red small balls — oxygen atoms).

Energy characteristics before and after sitting of ZnO nanoparticles of different dimensions

Number of atoms in nanoparticle	Number of atoms in super-cell	Full energy, eV/atom	Fermi energy, eV	Bond energy, eV	Charge on nanoparticle, e
0	273	-43.78	-4.32	—	—
6	279	-46.12	-4.57	-154.62	-0.131
12	285	-47.38	-4.68	-156.01	-0.403
48	321	-53.94	-4.86	-158.51	-0.799
96	369	-60.90	-4.93	-153.30	-0.791

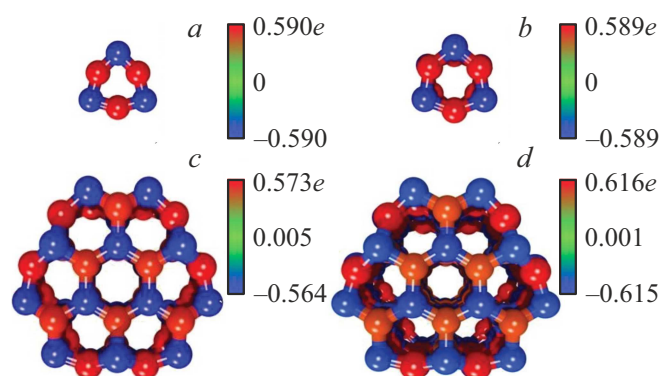


Figure 2. Maps of density distribution of electron charge by atoms of zinc oxide nanoparticle: *a*) 6 atoms, *b*) 12 atoms, *c*) 48 atoms, *d*) 96 atoms.

atoms to 96, see Figure 2, *d*, small difference occurs in values of positive charge (lack of charge) on zinc atoms. Now this value is within range $0.58 \pm 0.03e$. Lengths of bonds Zn–O are in range $2 \pm 0.02 \text{ \AA}$. Characteristic dimensions of maximum nanoparticles are: nanoparticle 48 atoms — $0.9 \times 0.96 \times 0.327 \text{ nm}$, 96 atoms — $1 \times 0.96 \times 0.7 \text{ nm}$. Thus, atomistic models of nanometer size are obtained, that can be used to study the process of AmGr decoration by them.

3.2. Adsorbing nanocrystals ZnO of different size on AmGr

The process of ZnO-nanoparticles adsorption was modeled as follows: nanoparticle was located in different local positions relative to NH-groups, namely 1) in direct vicinity of NH-groups, 2) on basal surface, and further optimization of super-lattice was performed with varying of all coordinates of all atoms (only lengths of translation vectors were fixed). As a result the most favorable position of the adsorbed nanoparticles on AmGr were identified. Figure 3 shows four cases of AmGr decoration by nanoparticles of 6, 12, 48 and 96 atoms. Types of super-cells, fragments of atomic structure, demonstrating contact ZnO+AmGr, and distribution of electron charge by atoms in contact region are presented. In all cases the localization of ZnO-nanoparticles near the amicogroups is optimal. At that covalent bonds Zn–N are formed in

three cases, when nanoparticles with number of atoms 12, 48 and 96 are adsorbed. Number of covalent bonds and their location are shown in inserts in Figure 3. Length of bond Zn–N in all cases is $2.06 \pm 0.02 \text{ \AA}$. Redistribution of electron charge density by atoms demonstrates obvious expression of charge flow in covalent bond Zn–N towards Zn-atom. In all other respects the pattern of density distribution of electron charge stays same for all ZnO-nanoparticles: maximum negative charge is concentrated in O-atoms of ZnO-nanoparticle, maximum of lack of electron charge is observed on Zn-atoms of same nanoparticle. The graphene atoms at that have small negative excessive charge within $-0.023 \pm 0.011|e|$ (in Figure 3 these atoms are marked with green color). Distance from graphene surface to nearest atoms of nanoparticles ZnO in all cases is approximately same and equal to $2.70 \pm 0.17 \text{ \AA}$. This spacing of nanoparticle relative to graphene corresponds to Van der Waals interaction. So, ZnO-nanoparticle is adsorbed on AmGr physically, at that forming partially also covalent bonds with graphene via nitrogen atoms.

Table presents metric, energy and electronic characteristics of all studied complexes „ZnO+AmGr“: number of atoms in super-cell, full energy (reduced to number of atoms), Fermi energy, ZnO–AmGr bond energy, and charge value transferred to ZnO-nanoparticle from AmGr surface.

Number of atoms in composition of super-cell increases from 273 to 369 as nanoparticle size increases. Full energy E_{tot} of complex „ZnO+AmGr“ appropriately decreases at that from value -43.782 to -60.899 eV/atom . Approximation of calculated results of full energy determined that its decreasing depending on size of ZnO-nanoparticle (number of atoms in nanoparticle — N) is described by quadratic function $E_{\text{tot}} = -45.079 + 2.026N - 1.038N^2$. This pattern, predictably, is true for rather low number of atoms in the nanoparticle: as the nanoparticle size increases the full energy would inevitably strive for saturation — i.e. strive to reach definite value — and, respectively, the nature of function of full energy would change. Change in fermi energy E_F also occurs as per quadratic law depending on number of atoms in the nanoparticle N : $E_F = -4.073 + 0.274N - 0.021N^2$. In this case, there is a clear tendency for the shift of Fermi energy value from zero towards decreasing. The bond energy has negative value, therefore, the adsorption process is energy favorable for all

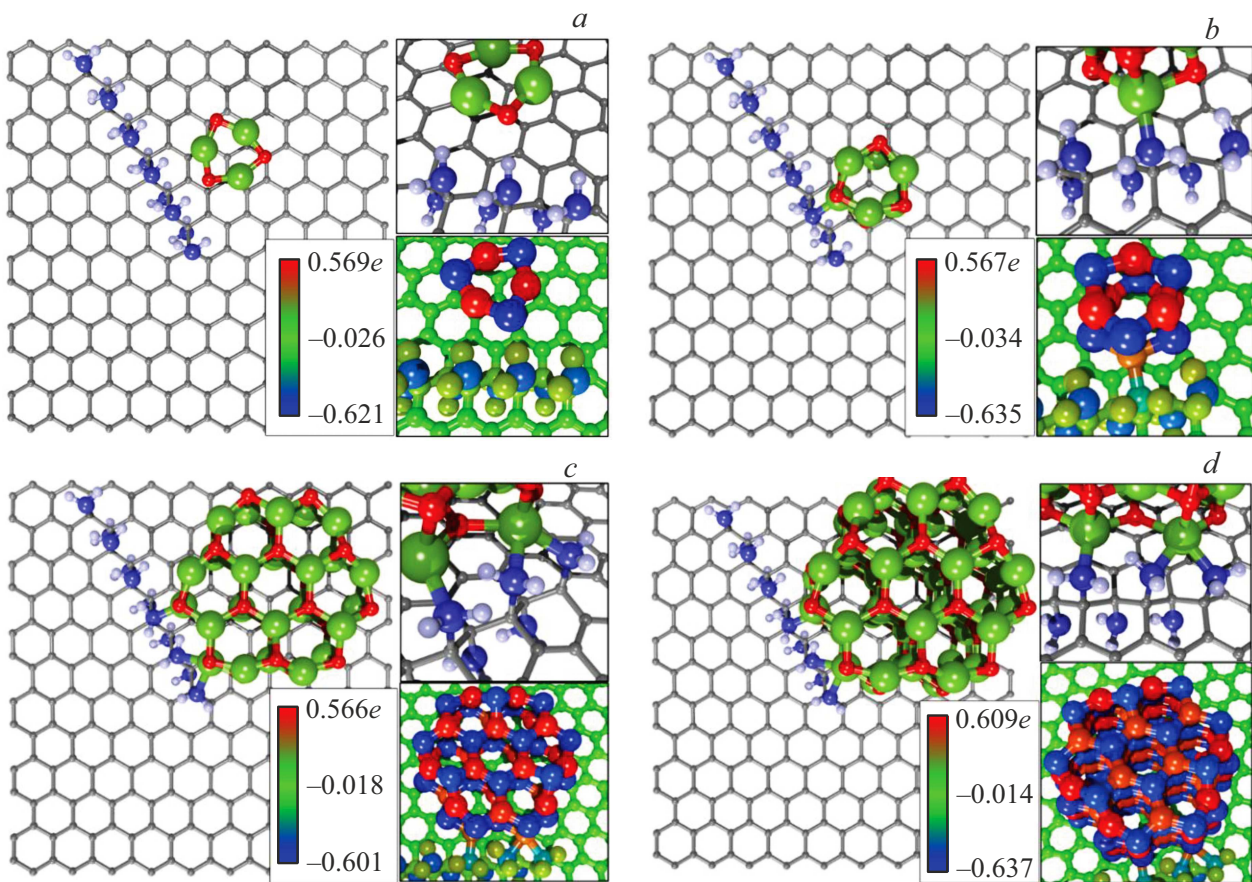


Figure 3. Atomistic models of super-cells AmGr and density distribution of electron charge during nanoparticle adsorption: with a) by 6 atoms, b) by 12 atoms, c) by 48 atoms, d) by 96 atoms.

deposited nanoparticles; in this case, the bond energy per atom of the nanoparticle remains practically constant and varies within the range 1.5%. During adsorption partial flow of charge on the nanoparticle from AmGr surface occurs. Charge value received by the surface reaches definite saturation and becomes equal to $\sim -0.79|e|$.

For all atomistic models „ZnO+AmGr“ functions of density of electron states (DoS) are calculated. For easy analysis and comparison the graphs in Figure 4 are given in normalized view (per number of atoms). It is clearly seen that at Fermi level in pure graphene value of density of electron states is zero, an in AmGr achieve local maximum, at the same time in all systems with different options of ZnO-nanoparticles adsorption on AmGr at fermi level increase in values of density of electron states is observed. So, for example, in case of sitting nanoparticle with six atoms value of density of electron states at Fermi level increases by 85.5% as compared to pure AmGr, in case of sitting the nanoparticle with 12 atoms — by 80.4%, in case of sitting nanoparticle with 48 atoms — by 87.2%, in case of sitting nanoparticle with 96 atoms — by 86.5%. Based on calculated functions DoS and their behavior at Fermi level we can suppose the nature of change in conductivity with increase in size of ZnO-nanoparticles adsorbed on AmGr.

By Figure 4 we can determine that after adsorption of ZnO-nanoparticles values of density of electron states increases near the fermi level, due to this the total conductivity increases.

Based on profile of function DoS, see above, the definite sup[ositions on conductivity were made. To check such suppositions and simultaneously evaluate prospects of such films „ZnO+AmGr“ as sensing elements of sensing devices the studies were performed relating pattern of quantum transport of electrons for AmGr upon presence on its surface of ZnO-nanoparticles of different size. Conductivity was calculated in direction „chair“ AmGr, because previously the authors demonstrated that exactly this direction is characterized by larger conductivity as compared to direction „zigzag“ [30]. Figure 5 presents calculated values of resistance for all cases of decoration by ZnO-nanoparticles. The results are presented in the form of bar diagram. Firstly value of electric resistance for pure AmGr upon absence of any ZnO-nanoparticle is provided. occurrence of lowest nanoparticle with six atoms (Figure 3,a) in local region AmGr practically does not change the conductivity of films „ZnO+AmGr“, which is quite expected in connection with the small value of the partial charge flow onto the nanoparticle and, at the same

time, the small shift in the Fermi energy. The adsorption of ZnO-nanoparticle with twelve atoms sharply changes the conductivity of film „ZnO+AmGr“, as result the electric resistance increases by three times and reaches maximum value 93.948 k Ω . This value is almost by three times higher than the resistance 32.9 k Ω for AmGr without ZnO-nanoparticles. Further, as number of atoms in nanoparticles increases, the resistance decreases, by insignificantly, i/e/ by 5–16%, see Figure 5. Naturally the issue arises on the reason of such abrupt rise of electric resistance, and by what physical reasons such phenomena can be explained.

To answer this question, additional studies were conducted on the interaction of nanoparticles with AmGr. Based on these studies the effect of influence of interatomic flow of electron charge on value of conductivity is identified. Analysis of value of flow electron charge showed that in case of lowest nanoparticle the charge value is $-0.022|e|/\text{atom}$ (6 atoms in ZnO-nanoparticle). Here the value of the charge flow is given related to the number of atoms in the nanoparticle, which simplifies the analysis of the obtained data. Upon increase in particle size from six atoms to twelve atoms there is abrupt increase in value of the charge flow AmGr–ZnO to value $-0.034|e|/\text{atom}$. At that all atoms of nanoparticle (naturally, oxygen atoms first of all) participate in charge flow from AmGr on nanoparticle regardless on number of atoms in contact with graphene surface. Said abrupt increase in value of charge flow from AmGr on nanoparticle resulted in abrupt decrease in conductivity, i.e. abrupt increase in electric resistance (Figure 5). Further with increase in ZnO-particles size to 48 and 96 atoms the electric resistance gradually decreases to 68.547 k Ω , this is expected, as with increase in number of atoms in nanoparticle they seem to screen each

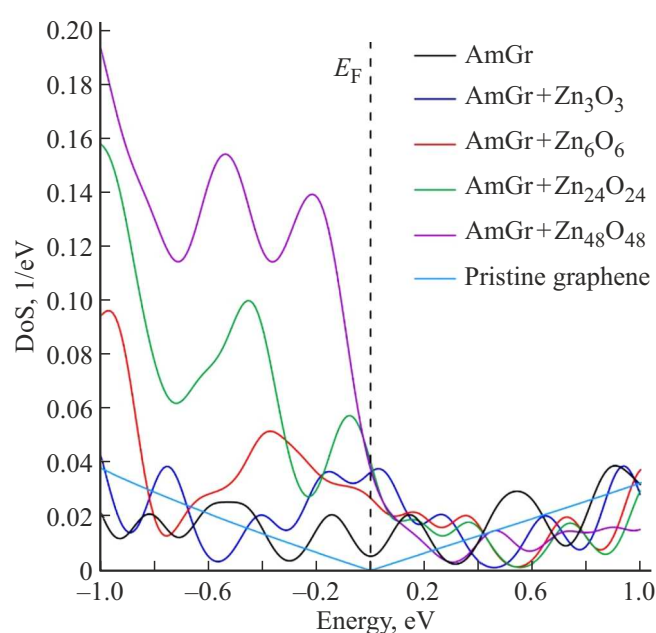


Figure 4. Graphs of DoS for four dimensions of nanoparticle, pure and aminated graphene.

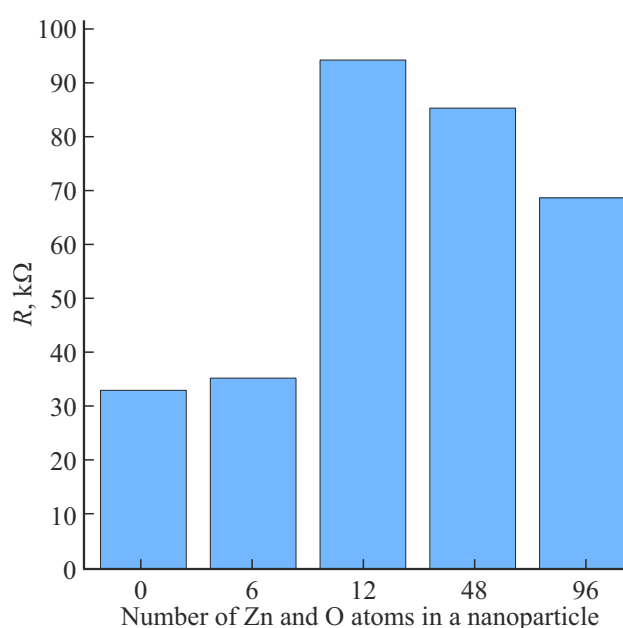


Figure 5. Resistance of AmGr before and after sitting ZnO-nanoparticles of different sizes.

other, and each atom, on average, takes only one charge $-0.03|e|/\text{atom}$ from electronic structure AmGr in case of nanoparticle of 48 atoms, and charge $-0.016|e|/\text{atom}$ — in case of nanoparticle of 96 atoms.

4. Conclusion

Using computer simulation with the density functional in the tight-binding approximation, the effect of decoration of aminated graphene with ZnO-nanoparticles on the density of electron states and conductivity is established. The effect of influence of nanoparticle size is determined. With increase in size of zinc oxide nanoparticle charge flows from AmGr surface on atoms of nanoparticles. Maximum charge flows on oxygen atoms of nanoparticle of 12 atoms. Pattern of effect of zinc oxide nanoparticles on conductivity of complex „AmGr+nanoarticle ZnO“ is established. Modification by AmGr nanoparticles results in resistance increasing by two-three times. Such films can be promising for sensorics as sensing element of gas detectors operating based on effect of chemoresistive response.

Funding

The work was performed within the framework of the State Assignment grant of the Ministry of Education and Science of the Russian Federation (project FSRR-2023-0008).

Conflict of interest

The authors declare that they have no conflict of interest.

References

- [1] A.J. Marsden, P. Brommer, J.J. Mudd, M.A. Dyson, R. Cook, M.C. Asensio, J. Avila, A. Levy, J. Sloan, D. Quigley, G.R. Bell, N.R. Wilson. *Nano Res.* **8**, 8, 2620 (2015).
- [2] P. Suvarnaphaet, S. Pechprasarn. *Sensors* **17**, 10, 2161 (2017).
- [3] L. Valentini, M. Cardinali, S.B. Bon, D. Bagnis, R. Verdejo, M.A. Lopez-Manchado, J.M. Kenny. *J. Mater. Chem.* **20**, 5, 995 (2010).
- [4] W. Zhang, J. Ma, D. Gao, Y. Zhou, C. Li, J. Zha, J. Zhang. *Prog. Org. Coat.* **94**, 9 (2016).
- [5] N. Krasteva, M. Keremidarska-Markova, K. Hristova-Panushcheva, T. Andreeva, G. Speranza, D. Wang, M. Draganova-Filipova, G. Miloshev, M. Georgieva. *Oxid. Med. Cell Longev.* **2019**, 1, 3738980 (2019).
- [6] M. Baraket, R. Stine, W.K. Lee, J.T. Robinson, C.R. Tamana, P.E. Sheehan, S.G. Walton. *Appl. Phys. Lett.* **100**, 23, 233123 (2012).
- [7] D.W. Boukhvalov. *RSC Adv.* **3**, 20, 7150 (2013).
- [8] D.W. Boukhvalov, M.I. Katsnelson. *J. Phys. Condens. Matter.* **21**, 34, 344205 (2009).
- [9] D.W. Boukhvalov, Y.-W. Son. *Nanoscale* **4**, 2, 417 (2012).
- [10] M. Wang, Z.B. Lai, D. Galpaya, C. Yan, N. Hu, L. Zhou. *J. Appl. Phys.* **115**, 12, 123520-1 (2014).
- [11] H. Al Mahmud, M.S. Radue, W.A. Pisani, G.M. Odegard. *Nanomater.* **11**, 11, 2919 (2021).
- [12] R.C. Sinclair, P.V. Coveney. *J. Chem. Inf. Model.* **59**, 6, 2741 (2019).
- [13] A. Lurf, H. He, M. Forster, J. Klinowski. *J. Phys. Chem. B* **102**, 23, 4477 (1998).
- [14] E. Aliyev, V. Filiz, M.M. Khan, Y.J. Lee, C. Abetz, V. Abetz. *Nanomater.* **9**, 8, 1180 (2019).
- [15] D.R. Dreyer, S. Park, C.W. Bielawski, R.S. Ruoff. *Chem. Soc. Rev.* **39**, 1, 228 (2010).
- [16] Y. Xu, G. Shi. *J. Mater. Chem.* **21**, 10, 3311 (2011).
- [17] S. Eigler, A. Hirsch. *Angew. Chem. Int. Ed.* **53**, 30, 7720 (2014).
- [18] M.K. Rabchinskii, S.A. Ryzhkov, D.A. Kirilenko, N.V. Ulin, M.V. Baidakova, V.V. Shnitov, S.I. Pavlov, R.G. Chumakov, D.Yu. Stolyarova, N.A. Besedina, A.V. Shvidchenko, D.V. Potorochin, F. Roth, D.A. Smirnov, M.V. Gudkov, M. Brzhezinskaya, O.I. Lebedev, V.P. Melnikov, P.N. Brunkov. *Sci. Rep.* **10**, 1, 6902 (2020).
- [19] O.E. Glukhova, M.K. Rabchinskii, S.D. Saveliev, D.A. Kirilenko, P.V. Barkov. *J. Compos. Sci.* **6**, 11, 335 (2022).
- [20] J.P. Liu, C.X. Guo, C.M. Li, Y.Y. Li, Q.B. Chi, X.T. Huang, L. Liao, T.Yu. *Electrochem. Commun.* **11**, 1, 202 (2009).
- [21] T. Yumak, F. Kuralay, M. Muti, A. Sinag, A. Erdem, S. Abaci. *Colloids Surf. B Biointerfaces* **86**, 2, 397 (2011).
- [22] Z. Li, Z. Zhou, G. Yun, K. Shi, X. Lv, B. Yang. *Nanoscale Res. Lett.* **8**, 1, 473 (2013).
- [23] S.H. Overbury, P.V. Radulovic, S. Thevuthasan, G.S. Herman, M.A. Henderson, C.H.F. Peden. *Surf. Sci.* **410**, 1, 106 (1998).
- [24] C.B. Duke, A.R. Lubinsky. *Surf. Sci.* **50**, 2, 605 (1975).
- [25] M. Sambì, G. Granozzi, G.A. Rizzi, M. Casarin, E. Tondello. *Surf. Sci.* **319**, 1–2, 149 (1994).
- [26] M. Galeotti, A. Atrei, U. Bardi, G. Rovida, M. Torrini, E. Zannazzi, A. Santucci, A. Klimov. *Chem. Phys. Lett.* **222**, 4, 349 (1994).
- [27] B. Hourahine, B. Aradi, V. Blum, F. Bonafé, A. Buccheri, C. Camacho, C. Cevallos, M.Y. Deshayé, T. Dumitrică, A. Dominguez, S. Ehlert, M. Elstner, T. van der Heide, J. Hermann, S. Irle, J.J. Kranz, C. Köhler, T. Kowalczyk, T. Kubař, I.S. Lee, V. Lutsker, R.J. Maurer, S.K. Min, I. Mitchell, C. Negre, T.A. Niehaus, A.M.N. Niklasson, A.J. Page, A. Pecchia, G. Penazzi, M.P. Persson, J. Řezáč, C.G. Sánchez, M. Sternberg, M. Stóhr, F. Stuckenberg, A. Tkatchenko, V.W.-z. Yu, T. Frauenheim. *J. Chem. Phys.* **152**, 12, 124101 (2020).
- [28] S. Datta. *Quantum Transport: Atom to Transistor*, 2nd ed. Cambridge University Press: N. Y., USA (2005). 420 p.
- [29] L.V. Keldysh. *JETP* **20**, 4, 1018 (1965).
- [30] O.E. Glukhova, P.V. Barkov. *Nanomater.* **2021**, 11, 1074 (2021).

Translated by I.Mazurov